Role of electron Coulomb interaction in superconductivity

H. Rietschel

Institut für Angewandte Kernphysik, Kernforschungszentrum Karlsruhe GmbH,
Postfach 3640, D-7500 Karlsruhe, Federal Republic of Germany

L. J. Sham

Department of Physics, University of California, San Diego, La Jolla, California 92093

The effect of the dynamically screened electron-electron interaction on the superconducting transition temperature is investigated by solving the Eliashberg equation in both frequency and momentum variables. The present calculations are performed within the random-phase-approximation (RPA)—screened free-electron model and for electronic density parameters $r_s < 5$. The full normal-state self-energy is included self-consistently. In parallel, the equation for the Coulomb pseudopotential μ^* is set up and solved using the imaginary-frequency representation. We find that in RPA plasmon exchange leads to a change in sign for μ^* at $r_s \sim 2.5$. For $r_s > 2.5$, $\mu^* < 0$ and the system becomes superconducting even without consideration of phonons. These results show that the effect of electron-electron attraction by plasmon exchange is overestimated in RPA, and that vertex corrections must be included. Similar conclusions have to be drawn for electron attraction through other high-frequency bosons such as excitons.

I. INTRODUCTION

If theory is to be of help in the search for superconductors with high transition temperatures T_c, it has to possess the capability of predicting T_c from first principles better than at present. Despite the enormous progress made in the last decade in the microscopic theory of superconductivity, reliable prediction of T_c remains a problem.[1-3] Since the basic equations for determining T_c, viz., the Eliashberg equations,[4,5] are held to provide T_c within 1% or better, and since the solution of these equations is also capable of accuracy to within a few percent,[2] the source of errors is traced to the normal-state properties which are inputs to the Eliashberg equations. These consist of the electron band structure, the phonon spectrum, the electron-phonon interaction, and the Coulomb repulsion between electrons. The focus of this paper is on the last item.

Because of the enormous difference between the phonon and electron energies in most metals, it is advantageous to solve the Eliashberg equations in two steps by dividing the ω space into two regions.[2,4,5] For frequencies below, say, $\omega_0 \sim 5\omega_D$ (ω_D being the Debye frequency) and momenta near the Fermi surface, the formation of the Cooper pair is dominated by the electron-phonon-electron interaction modified by the effects of Coulomb interaction between electrons, which can be characterized for a given cutoff ω_0 by a single number μ^*. In this region, the reduced Eliashberg equation may be solved by the usual simplifications made possible by the Migdal theorem.[2] μ^* is determined by the solution of the Eliashberg equation outside the phonon frequency range, namely greater than ω_0. There, the dynamically screened Coulomb interaction between the

electrons has to be taken into account, which excludes further use of Migdal's theorem. Consequently, the solutions for the self-energy now depend on both frequency and momentum, and vertex corrections may become important.

In principle, μ^* can be determined from measurements, such as the isotope effect[6] and the tunneling spectra.[7] However, the availability of measured values of the isotope shift of T_c is limited to some elements and a few compounds, and a certain amount of uncertainty in the derived values of μ^* arises by the so-called indirect isotope effect.[8] Similarly, the tunneling data are restricted to a few materials, and there is also uncertainty in the extraction of μ^*. From these considerations, the value of 0.13 for μ^* in transition metals of 0.10 in simple metals have become widely adopted. It has recently become evident that in some materials, such values of μ^* do not adequately represent the effects of the electron Coulomb interaction. In some materials, such as compounds of vanadium, the calculated T_c is too high compared with the measured T_c. Since the error is significantly larger than that estimated for the electron-phonon interaction,[9] it leads to the conclusion that μ^* must exceed 0.1 considerably, mainly because of the pair-breaking influence of spin fluctuations.[10] On the other hand, it has been suggested that plasmons, particularly acoustic plasmons, could reduce μ^* or even render it negative, i.e., sustain superconductivity without phonons.[11,12] There have also been suggestions[13] that proximity of semiconductor band structure can create in a metal excitonlike excitations which would lead to very high T_c.

All these excitations—plasmons, acoustic plasmons, and excitons—which are suggested as more potent replace-

ments for the phonons, can be grouped together with spin fluctuations as various manifestations of the frequency dependence of the effective electron-electron interaction. The solution of the Eliashberg equation with a given effective electron-electron interaction, therefore, deserves careful study. The common practice of estimating the strength of the electron repulsion which determines μ^* by averaging a statically screened Coulomb interaction over the Fermi surface is clearly inadequate. An approximation by Kirzhits, Maksimov, and Khomskii[14,13] (KMK) which converts the ω and k dependence of the Eliashberg equation into an equation with only k dependence, is frequently used for estimating T_c due to nonphonon mechanisms.[12,13,15] However, it has been shown[16] that, in the weak coupling limit, where the KMK approximation is supposed to be valid, an important term has been left out which vitiates the resulting T_c estimate. For the electron-interaction model considered in this paper, the KMK approximation fails completely.

In this paper, we adopt the random-phase approximation (RPA) for the electron interaction in the jellium model. Thereby, the polarizability of the positive background is neglected, i.e., no phonons are considered in this model. The attractive interaction due to the plasmons serves as a paradigm for the various attraction mechanisms at high frequencies, proposed in the literature. The dielectric formulation takes care of the delicate balance between the attractive part (the collective mode) and the original repulsive nature of the Coulomb interaction. The order parameter in the Eliashberg equation is calculated as a function of ω and k. As far as we know, this is the first time both ω and k dependence are taken into account simultaneously. The resultant μ^* for the electron gas as a function of r_s serves as a first approximation for simple metals. The paper is organized as follows. In Sec. II, the Eliashberg equations for T_c are given, together with a short description of the numerical procedures for their solution. In Sec. III, the variation of eigenfunctions of the gap equation with both momentum k and frequency ω is discussed, with particular emphasis on their nodes and dependence on the structure of the interaction. In Sec. IV, the contribution of the Coulomb interaction to the Eliashberg equation is reduced to an equation for the pseudopotential ξ^*. An exactly soluble square-well model is used to illustrate the delicate balance between the static Coulomb repulsion and the dynamic Coulomb attraction due to plasmon exchange. Section V presents the numerical results when the RPA is used for the Coulomb interaction. We start this section by discussing our results for the normal-state properties: renormalization constant Z, effective-mass ratio m^*/m, and correlation potential ξ_c. These quantities are important ingredients in the equation for μ^*. Moreover, they offer a valuable check of our calculations by comparing them to earlier results of other authors. Our findings for μ^* and T_c show that the RPA favors superconductivity too much, which means that (i) using the RPA in nonphonon mechanisms, in general, tends to overestimate T_c and that (ii) corrections beyond the RPA are important. Section VI contains a summary of our findings and a discussion of the future direction of our investigation.

II. ELIASHBERG EQUATIONS AND NUMERICAL TREATMENT

Since our considerations of superconductivity are restricted to T_c, only the Eliashberg equations linearized in the gap function are needed. In an imaginary frequency representation and for isotropic systems they are written as[5]

$$\phi_n(k) = -T \sum_{m=-\infty}^{\infty} \int_0^\infty dk' k'^2 V^-(k,k';v_{nm})$$
$$\times G_m(k')\phi_m(k') , \tag{1a}$$

$$\omega_n - \omega_n(k) = T \sum_{m=-\infty}^{\infty} \int_0^\infty dk' k'^2 V^+(k,k';v_{nm})$$
$$\times G_m(k')\omega_m(k') , \tag{1b}$$

$$\chi_n^c(k) = T \sum_{m=-\infty}^{\infty} \int_0^\infty dk' k'^2 [V^+(k,k';v_{nm}) - V_0(k,k')]$$
$$\times G_m(k')\epsilon_m(k') , \tag{1c}$$

$$\Delta\chi^{ex}(k) = \int_0^\infty dk' k'^2 V_0(k,k')T$$
$$\times \sum_m [\epsilon_m(k')G_m(k') - \epsilon_0(k')\widetilde{G}_m(k')] , \tag{1d}$$

$$\chi_0^{ex}(k) = \int_0^\infty dk' k'^2 V_0(k,k') \left[-\frac{1}{2} + T \sum_m \epsilon_0(k')\widetilde{G}_m(k') \right] . \tag{1e}$$

Here, we use the following abbreviations:

$$G_n(k) = 1/[\omega_n^2(k) + \epsilon_n^2(k)] , \tag{2a}$$

$$\widetilde{G}_n(k) = 1/[\omega_n^2 Z_0(k)^2 + \epsilon_0^2(k)] , \tag{2b}$$

$$\epsilon_n(k) = k^2 + \chi_n(k) - \xi , \tag{2c}$$

$$\omega_n = (2n+1)\pi T , \quad v_{nm} = \omega_n - \omega_m , \tag{2d}$$

$$\omega_n(k) = \omega_n Z_n(k) . \tag{2e}$$

$\phi_n(k)$ is the momentum- and frequency-dependent gap function, and $[\omega_n - \omega_n(k)]$ is the odd part of the normal-state self-energy, while its even part $\chi_n(k)$ has been decomposed into

$$\chi_n(k) = \chi_n^c(k) + \chi_0^{ex}(k) + \Delta\chi^{ex}(k) . \tag{3}$$

$\chi_n^c(k)$ comes from the correlation part of the self-energy diagrams and $\chi_0^{ex} + \Delta\chi^{ex}$ from the exchange diagram with the intermediate states renormalized. Were the renormalization neglected as in common practice, the exchange part would reduce to

$$\chi_{00}^{ex}(k) = -4\alpha \left[\frac{k^2-1}{4k} \ln \left| \frac{k+1}{k-1} \right| + \frac{1}{2} \right] \quad \text{at } T=0 \tag{4}$$

with $\alpha = 1/\pi k_F a_B = r_s/6.03$, the Coulomb coupling constant.

If not stated otherwise, energies and temperatures are measured in units of ϵ_F and momenta in units of k_F. ξ is the chemical potential which at $T=0$ is given by

$$\xi = 1 + \mathcal{X}_0^{\text{ex}}(k_F) + \Delta\mathcal{X}^{\text{ex}}(k_F) + \xi_c \ , \quad \xi_c = \mathcal{X}^c(\omega=0,k_F)$$

(5)

where $\mathcal{X}^c(\omega,k_F)$ is the analytical continuation of $\mathcal{X}_n^c(k_F)$ onto the real axis. For low temperatures, $\xi_c \sim \mathcal{X}_0^c(k_F)$. The potentials $V^\pm(k,k';\nu)$ and $V_0(k,k')$ are given by

$$V^\pm(k,k';\nu) = \frac{1}{4\pi^2 kk'} \int_{|k-k'|}^{k+k'} dq\, q V^\pm(q,\nu) \ ,$$

(6)

$$V_0(k,k') = \frac{2\alpha}{kk'} \ln\left| \frac{k+k'}{k-k'} \right| \ ,$$

(7)

where $V^-(q,\nu)$ is the Cooper-pair interaction and $V^+(q,\nu)$ the interaction entering the normal-state self-energy. $V_0(k,k')$ is the s-wave average over the bare Coulomb interaction, and since (6) also represents an s-wave average, our solutions will be restricted to s-wave pairing. In general, V^+ and V^- are different because of the spin dependence of the four-point vertex. Within the RPA, V^+ and V^- are equal and given by[17]

$$V_{\text{RPA}}(k,k';\nu) = \frac{2\alpha}{kk'} \int_{|k-k'|}^{k+k'} \frac{dq}{q} \frac{1}{1+F(q,\nu)} \ ,$$

$$F(q,\nu) = \frac{2\alpha}{q^3} \int_0^1 dk\, k \ln\left| \frac{\nu^2 + (2kq + q^2)^2}{\nu^2 + (2kq - q^2)^2} \right| \ .$$

(8)

In order to perform the unlimited summations over m and integrations over k', the proper knowledge of the asymptotic limits for $\phi_n(k)$, $\omega_n(k)$, and $\mathcal{X}_n(k)$ is required. We summarize the power laws which can easily be derived within the RPA as follows:

$$\phi_n(k) \sim \begin{cases} \phi_\infty(k) \ , & n \to \infty \\ c/k^2 \ , & k \to \infty \end{cases}$$

(9a)

$$\omega_k - \omega_n(k) \sim \begin{cases} 1/\omega_n \ , & n \to \infty \\ 1/k^4 \ , & k \to \infty \end{cases}$$

(9b)

$$\mathcal{X}_n^c(k) \sim \begin{cases} 1/\omega_n^{3/2} \ , & n \to \infty \\ 1/k^2 \ , & k \to \infty \end{cases}$$

(9c)

$$\mathcal{X}_0^{\text{ex}} + \Delta\mathcal{X}^{\text{ex}}(k) \sim 1/k^2 \ , \quad k \to \infty \ .$$

(9d)

Restricting the arguments of the left-hand sides of Eqs. (1) to $\omega_n \sim \omega_p$ [$\omega_p = (4\pi e^2 N/m)^{1/2}$], $k \sim k_F$, we find for the right-hand sides

$$k'^2 V^-(k,k';\nu_{n,m}) G_m(k')\phi_m(k') \sim \begin{cases} 1/\omega_m^2 \ , & m \to \infty \\ 1/k'^6 \ , & k' \to \infty \end{cases}$$

(10a)

$$k'^2 [V^+(k,k';\nu_{n,m}) - V^+(k,k';\nu_{n,-m})]G_m(k')\omega_m(k')$$
$$\sim \begin{cases} 1/\omega_m^4 \ , & m \to \infty \\ 1/k'^{12} \ , & k' \to \infty \end{cases}$$

(10b)

$$k'^2 [V^+(k,k';\nu_{n,m}) - V_0(k,k')]G_m(k')\epsilon_m(k')$$
$$\sim \begin{cases} 1/\omega_m^4 \ , & m \to \infty \\ 1/k'^6 \ , & k' \to \infty \end{cases}$$

(10c)

$$k'^2 V_0(k,k')[G_m(k')\epsilon_m(k') - \widetilde{G}_m(k')\epsilon_0(k')]$$
$$\sim \begin{cases} 1/\omega_m^2 \ , & m \to \infty \\ 1/k'^4 \ , & k' \to \infty \end{cases}$$

(10d)

and, with

$$\frac{1}{2} - T\sum_m \epsilon_0(k')\widetilde{G}_m(k') = \frac{1}{2} - \frac{1}{2Z_0(k')} \tanh\frac{\epsilon_0(k')}{2TZ_0(k')} \equiv n_{k'}^0$$

for Eq. (1e), it follows that

$$-k'^2 V_0(k,k')n_{k'}^0 \sim 1/k'^4 \ , \quad k' \to \infty \ .$$

(10e)

In Eq. (10b) the fact has been exploited that $\omega_n(k)$ is an odd function in n. Except for the $1/\omega_m^2$ decrease in (10a) and (10d), all other power laws provide excellent convergence and allow for low-lying cutoffs ω_c and k_c. In our calculations, $\omega_c = 3\omega_p$ and $k_c = 3$ proved sufficient to guarantee a relative accuracy of 10^{-2} or better for both pseudopotentials μ^* and eigenvalues λ of the gap equation, while $\omega_c = 5\omega_p$ and $k_c = 4$ were required to provide the same accuracy for the normal state properties $Z_0(k_F)$, m^*/m, and μ_c (see below). Equations (1a) and (1d) cannot be cut off at ω_c. Instead, we set $Z_n^{(k)} = 1$, $\mathcal{X}_n^c(k) = 0$, and $\phi_n(k) = \phi_\infty(k)$ for $\omega_n > \omega_c$, and we transformed the m sums into integrals which were carried out explicitly to infinity.

A further problem is presented by k being a continuous variable. We subdivided $[0,k_c]$ into n_k sections, assuming the self-energy to be constant within each section. A direct measure of the quality of this approach is the convergence of the results for increasing n_k. $n_k = 50$ was required for the evaluation of the derivative $d\epsilon_n(k)/dk$ and for the determination of μ_c. For all other quantities, $n_k = 10$ is sufficient. Thus, for the normal-state self-energy we used $n_k = 50$, while for the solution of the gap equation and pseudopotential equation, respectively, $n_k = 10$ was taken. Raising n_k from 10 to 30 resulted in relative changes of λ and μ^* (see below) of order of or less than 10^{-2}.

Care must be taken for a proper treatment of the logarithmic singularity in $V^\pm(k,k';\nu)$ at $k=k'$. We extracted this singularity and integrated it analytically, keeping the remaining factors constant in a small neighborhood around the singularity. A similar procedure was applied to $G_m(k)$ which is sharply peaked for small ω_m and $k \to 0$.

Equations (1a)–(1e) are solved by iteration. For a given T, Eqs. (1b)–(1e) are solved first. Once $\omega_m(k)$ and $\mathcal{X}_n(k)$ have been calculated, Eq. (1a) is cast into an eigenvalue equation by multiplying it on the left-hand side with the eigenvalue λ. In self-explanatory notation,

$$\lambda\vec{\phi} = -V^-\hat{G}\vec{\phi} \ ,$$

(11)

where $\lambda = \lambda(T)$. Equation (11) is solved for λ, again by iteration. Since a superconducting transition is now characterized by $\lambda(T_c) = 1$, we repeat the cycle for different T in order to find $\lambda = 1$.

The iteration of an eigenvalue equation leads to convergence towards the dominant eigenvalue (the one with largest absolute value). The physical eigenvalue λ_p which we

are interested in, is the largest with positive sign, but is always smaller in absolute value than at least one other eigenvalue λ_1, which is very large and negative, and sometimes smaller than a second eigenvalue λ_2, also negative in sign. We overcame this difficulty by using a 3×3 representation of the gap equation, starting with three trial functions orthogonal to each other and diagonalizing the iterated eigenfunctions after each step.

The procedure described in the last paragraphs turned out to be practicable for $T \gtrsim 0.01$ only. If T drops below this value, the increasing number of frequencies ω_m will quickly render the calculations too time consuming. Actually, we used this approach only for $T \gtrsim 0.05$ and for qualitative investigations of the structure of the eigenfunctions. For $T \lesssim 0.05$ and for practical purposes (calculation of T_c or μ^*), the pseudopotential method described in Sec. IV turned out to be much faster and more elegant.

III. STRUCTURE OF THE GAP FUNCTION IN THE RPA

We now study the k and ω_n dependence of the self-energy in the RPA, laying particular stress on the gap function $\phi_n(k)$. We illustrate this discussion by explicit calculations for the following set of parameters: $r_s = 4$, $T = 0.05$ (again in units of ϵ_F), and defer the discussion of T_c, μ^*, and the normal-state self-energy to Sec. V.

The first three dominating eigenvalues of Eq. (11) are $\lambda_1 = -2.82$, $\lambda_2 = -0.70$, and $\lambda_p = +0.63$. The last eigenvalue is the physical one, tending to 1 for $T = 3\times10^{-4}$, thus driving the system superconducting. The corresponding eigenfunctions are presented in Figs. 1 and 2 as functions of both k and ω_n. Here, $n = 0$ and $k = 1.05$, respectively, have been used, with the exception of $\vec{\phi}_{\lambda_2}$, where $k = 0.75$ has been used instead (this eigenfunction is almost zero near k_F).

From the fact that all matrix elements of $\hat{V}^- \hat{G}$ in (11) are positive it immediately follows that $\vec{\phi}$ has to have at least one line of nodes in the k, ω_n plane to produce a positive eigenvalue. If $\hat{V}^-$ were without structure, i.e., without k and ω_n dependence, so would be $\vec{\phi}$ and no positive eigenvalue could appear. Thus, it is evident that structure in $\hat{V}^-$ is necessary to yield superconductivity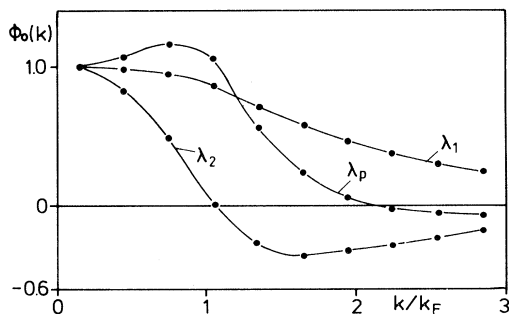 in a system with completely repulsive interaction. The question is now, where the nodes of $\vec{\phi}$ are. The eigenfunction $\vec{\phi}_{\lambda_1}$ has no node, either in ω_n or in k. It represents the "ground state" of the system with the largest negative, and therefore unphysical, eigenvalue λ_1. λ_2 again is negative, but $\vec{\phi}_{\lambda_2}$ has a node in k near k_F. The physical eigenvalue λ_p is accompanied by a $\vec{\phi}_{\lambda_p}$ which has a node in ω_n at about $0.6\omega_p$. It also has a node in k around 2, but according to Eq. (9a) this is already in a region which contributes slightly to λ_p. From these findings it becomes clear that structure of $\hat{V}^-$ in ω_n is decisive for the possible occurrence of superconductivity in the system under consideration. So, any type of approximation to Eqs. (1) which neglects or averages structure in ω_n is not applicable to our system.

We conclude this section by analyzing the shape of the Cooper pair interaction $V^-(k,k';\nu)$ for the RPA as given by Eq. (7). As has been discussed in the preceding section, in the numerical treatment the logarithmic singularity at $k'=k$ has been removed by integrating k' over the corresponding k section. In Fig. 3 we show this coarse grain averaged potential $\langle V(k,k';\nu)\rangle$ as a function of ν and for $k,k'=0.9$. Qualitatively, these potentials can well be approximated by
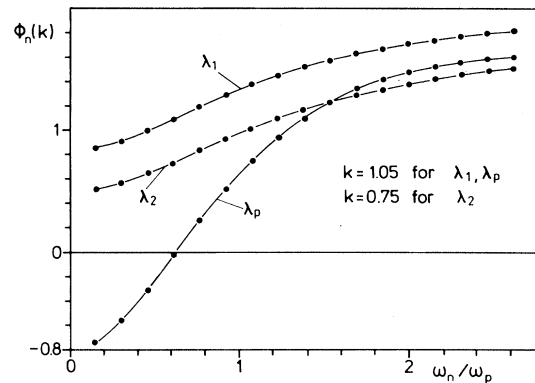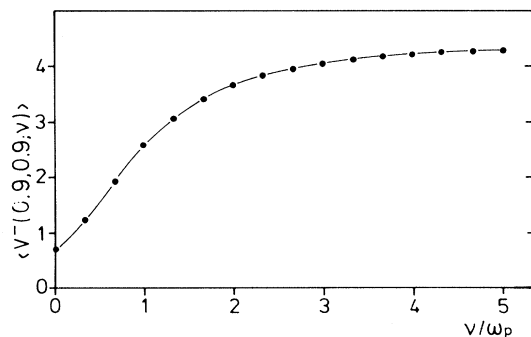

FIG. 2. Gap functions $\phi_n(k)$ vs ω_n at $k = 1.05$ for $\lambda = \lambda_1, \lambda_p$ and at $k = 0.75$ for $\lambda = \lambda_2$.

FIG. 1. Gap functions $\phi_n(k)$ vs k at $n = 0$ associated with the three eigenvalues largest in absolute magnitude.

FIG. 3. Imaginary frequency dependence of the effective electron interaction, coarse grain averaged in k space at $k = 0.9 = k'$.

$$\langle V^-(k,k';\nu)\rangle \sim f(k,k') \left[1 - \sigma(k,k') \frac{\omega_p^2}{\nu^2 + \omega_p^2} \right] . \tag{12}$$

Of course, (12) is not used in the calculations, but it demonstrates the well-known fact that V^- is made up of two components, a static repulsive part and an attractive part due to exchange of virtual plasmons. This latter part leads to a depression of $\langle V^-(k,k';\nu)\rangle$ for $\nu \to 0$, its strength being given by $\sigma(k,k')$. As will be discussed in the following chapter, this depression is of vital importance for the possible occurrence of superconductivity, and μ^* and T_c are extremely sensitive to changes in $\sigma(k,k')$. A plot of $\sigma(k,k)$ which in general terms is defined by

$$\sigma(k,k) = \frac{[\langle V^-(k,k;\infty)\rangle - \langle V^-(k,k;0)\rangle]}{\langle V^-(k,k;\infty)\rangle} \tag{13}$$

is shown in Fig. 4.

IV. PSEUDOPOTENTIAL

Since the pseudopotential approach has been discussed considerably in the literature,[4,5] we will just sketch what we need. The basic idea consists in separating the frequency dependence into two ranges, below and above a cutoff ω_0, which is chosen to be large enough to include all the phonon effects but also small enough to be below the scale of E_F or ω_p. In the frequency range below ω_0, the k dependence of the gap function may be removed by confining k to the Fermi surface, and the Coulomb interaction between electrons reduces to a pseudopotential μ^*. The contribution of the direct electron-electron interaction to μ^* is obtained by solving the Eliashberg equation above ω_0 [see Eq. (19)].

Before proceeding with this, let us consider a simple but instructive model, with the following gap equation:

$$\phi_n = -T \sum_m K_{n,m} \int_{-1}^1 d\epsilon \frac{1}{\omega_m^2 + \epsilon^2} \phi_m , \tag{14}$$

where

$$K_{n,m} = \begin{cases} \mu(1-\sigma) & |\omega_n| \le \omega_p , \ |\omega_m| \le \omega_p \\ \mu & \text{otherwise} . \end{cases} \tag{15}$$
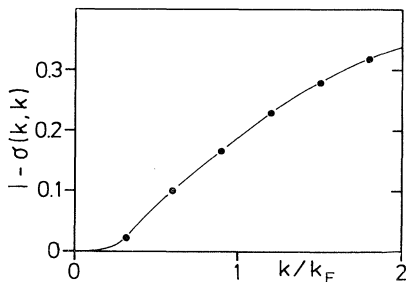

FIG. 4. Coefficient of attraction from Eq. (12), $\sigma(k,k)$ vs k.

$K_{n,m}$ represents a square-well potential with a fractional depression σ, roughly modeling the screened Coulomb interaction in Eq. (12). Equation (14) can be solved trivially. If a cutoff ω_0 is deliberately introduced, the transition temperature assumes the form

$$T_c = 1.13\omega_0 \exp(1/\mu_m^*) , \tag{16}$$

with

$$\mu_m^* = -\tilde{\mu}/[1 + \tilde{\mu}(f + \ln\omega_0)] , \tag{17a}$$

$$\tilde{\mu} = \mu\sigma - \frac{\mu}{1+\mu f} , \tag{17b}$$

$$f = T \sum_{|\omega_m| > |\omega_p|} \frac{2}{\omega_m} \tan^{-1}(1/\omega_m) . \tag{17c}$$

μ_m^* is identified as the pseudopotential of our model, and clearly depends on the choice of the cutoff ω_0 whereas T_c does not.

The condition for the occurrence of superconductivity is

$$\mu_m^* < 0 \quad \text{or} \quad \sigma > (1+\mu f)^{-1} . \tag{18}$$

The depression of the well has to be sufficiently large for superconductivity to exist, i.e., there is a *critical* value for σ below which no superconductivity can occur. This important statement is also true for the more general k and ω dependent interaction $\langle V^-(k,k';\nu)\rangle$, and it is the particular virtue of the simplified model to preserve this feature.

Whenever σ is close to $1/(1+\mu f)$, μ_m^* and T_c react very sensitively to any change in σ. As will be demonstrated by our numerical results in the next section, it is just this situation we are dealing with in the case of Coulomb interaction. There, static repulsion and dynamic attraction are almost in balance, and any approximation affecting this balance will lead to severe errors.

Returning to the pseudopotential equation for the more general interaction, we make use of the discrete k representation discussed in Sec. III and write the gap equation (1a) in the following way:

$$\phi_n(k_i) = \sum_j \sum_{|m| \le m_0} K_{n,m}^{i,j} S_m^j \Phi_m(k_j)$$
$$+ \sum_j \sum_{|m| > m_0} K_{n,m}^{i,j} S_m^j \Phi_m(k_j) ,$$

$$K_{n,m}^{i,j} = -T\Delta \frac{k_j}{2} V^-(k_i,k_j;\nu_{n,m}) , \quad S_m^j = 2k_j G_m(k_j) \tag{19}$$

where $\Delta = k_c/n_k$ is the width of the k intervals and $\omega_0 = (2m_0+1)\pi T$. In matrix notation, (19) can be written as

$$\vec{\phi} = \hat{K}_1 \hat{S} \vec{\phi} + \hat{K}_2 \hat{S} \vec{\phi} , \tag{20}$$

where $\hat{K}_1$ is the part of the matrix $\hat{K}$ with columns $|m| > m_0$ replaced by zeros, and $\hat{K}_2$ is the complementary part of K. Equation (20) can be rearranged to give

$$\vec{\phi} = \hat{C}\hat{S}\vec{\phi} , \tag{21}$$

$$\hat{C} = (1 - \hat{K}_2 \hat{S})^{-1} \cdot \hat{K}_1 \ . \qquad (22)$$

Since $K_{1n,m}^{i,j} = 0$ for $|m| > m_0$, the m sum on the right-hand side of Eq. (21) is restricted to $|m| \leq m_0$ or $|\omega_m| < \omega_0$, and S acts as a δ function for $k_j = k_F$. The summation over k_j (integration over k') can be carried through, and we are left with

$$\phi_n(k_i) = \sum_{|m| < m_0} \frac{1}{ZD} C_{n,m}^{k_i,k_F} \frac{\pi}{|\omega_m|} \phi_m(k_F) \ . \qquad (23)$$

For $\omega_0 \ll \omega_p$, $C_{n,m}^{k_i k_F}$ is independent of n, m for $|\omega_n|, |\omega_m| \leq \omega_0$, and so is $\phi_n(k_j)$. Restricting k_i to $k_i = k_F$, we finally get

$$1 = -T\mu^* \sum_{|m| < m_0} \frac{\pi}{|\omega_m|} \ , \qquad (24)$$

$$\mu^* = -\frac{1}{T} C_{00}^{k_F k_F} \frac{1}{ZD} \ , \qquad (25)$$

$$Z = Z_0(k_F) \ , \quad D = 1 + \frac{1}{2k_F} \frac{\partial \epsilon_0(k)}{\partial k}\bigg|_{k = k_F} \ . \qquad (26)$$

The calculation of μ^* from (25) requires the solution of (22), i.e., the inversion of the matrix $(1 - \hat{K}_2 \hat{S})$. In k space, this matrix is of dimension $n_k \sim 10$. Since $T_c \ll 1$ in all realistic situations where μ^* is to be used, in ω_n space we assumed a quasicontinuum which was summed over from ω_0 to ω_c by means of a Simpson integral procedure. Typically 15–25 points were used with decreasing spacing for decreasing ω_n, resulting in a relative error in μ^* of about 10^{-2}. Above ω_c we summed ω_n explicitly in exactly the same way as when solving the gap equation (see Sec. III). Thus, the overall dimension of the matrix to be inverted is about 150–250, which represents no problem on a modern computer. The normal-state self-energy which enters $\hat{K}_1$ and $\hat{K}_2$, has been calculated for $T = 0.05$ throughout, which represents an excellent approximation to the $T \sim 0$ values we actually need. Changes in these quantities when decreasing T further to $T = 0.01$, turned out to be completely negligible.

V. NUMERICAL RESULTS

Our numerical solutions have been generated by using dressed Green's functions in the irreducible self-energy parts in Eqs. (1), which is achieved by iteration. In what follows, we will designate this self-consistent treatment of the RPA as the SRPA. Typically, five to ten iteration steps are sufficient to keep the relative changes in the self-energy below 10^{-2} for two successive steps. For reasons of comparison to results already quoted in the literature, we also performed calculations starting with undressed Green's functions and stopped after the first iteration step. Following common usage this will be called the RPA.

We first present the normal-state self-energy. Explicitly, it enters μ^* by the product ZD via Eq. (25). Z and D are given in Table I for both the RPA and SRPA. Hedin[18] has published RPA results for Z which are in excellent agreement with our RPA results.

Whereas Z and D enter μ^* as a product, the effective mass m^* is determined by their ratio,

$$m^*/m = Z/D \ . \qquad (27)$$

For $r_s \leq 5$ we find m^*/m close to 1 and approaching the high-density evaluation of Du Bois[19] for $r_s < 1$ (see Fig. 5) in both the RPA and SRPA. But in the RPA, $m^*/m - 1$ changes sign at $r_s \sim 3$, while in the SRPA, m^*/m is slightly depressed and always below 1.

The full ω_n and k dependence of the normal-state self-energy enters T_c and μ^*, respectively, implicitly via Eq. (1a) and Eqs. (22) and (25), respectively. In Figs. 6–8, $\chi_n(k)$ and $Z_n(k)$ are shown as functions of ω_n and k, respectively. Again, $r_s = 4$ and $T = 0.05$ have been chosen together with $k = k_F$ and $n = 0$, respectively, as representative examples.

The last normal-state quantity to be discussed is ξ_c, the correlation contribution to the chemical potential. Since ξ_c and the correlation part E_c of the ground-state energy are related by[20]

$$\xi_c = E_c - \frac{r_s}{3} \frac{\partial E_c}{\partial r_s} \ , \qquad (28)$$

TABLE I. Normal-state properties Z, D, and ξ_c, and superconducting properties μ^* and T_c of the free-electron gas in the RPA and SRPA; μ^* values are defined for a cutoff of $\omega_0 = 1000$ K; effective mass defined by $m^*/m = Z/D$.

r_s		0.25	0.5	1	2	3	4	5
Z^a		1.038	1.075	1.139	1.247	1.335	1.411	1.477
Z^b		1.041	1.081	1.158	1.302	1.435	1.561	1.680
Z^c				1.164	1.302	1.429	1.548	1.661
D^a		1.072	1.122	1.205	1.343	1.466	1.582	1.695
D^b		1.073	1.123	1.203	1.330	1.438	1.537	1.629
ξ_c^a		−0.004	−0.013	−0.046	−0.148	−0.272	−0.426	−0.597
ξ_c^b		−0.004	−0.013	−0.045	−0.144	−0.280	−0.446	−0.637
ξ_c^d				−0.047	−0.15	−0.29	−0.47	−0.65
μ^* (1000 K)^a				0.045	0.022	−0.018	−0.066	−0.12
T_c (K^{-1})						$\sim 10^{-22}$	3×10^{-4}	0.22

^{a}Present calculation (SRPA).
^{b}Present calculation (RPA).
^{c}Reference 18.
^{d}Reference 21.
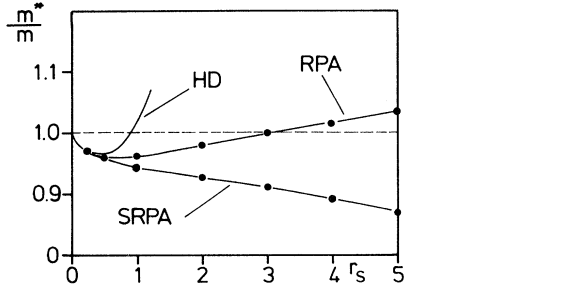
FIG. 5. Effective mass vs r_s. HD: high-density evaluation of Ref. 19.

FIG. 7. Odd part of the normal-state self-energy vs k for $n = 0$.

our results may be compared to published results for E_c as those given by Vosko et al.[21] for the RPA. From their data we calculated $\partial E_c / \partial r_s$ by fitting $E_c(r_s)$ with a suitably chosen function and determining its derivative analytically. These ξ_c values are compared to ours in Table I. In the RPA, our results are lower by a few percent, a difference which could be reduced by increasing k_c and ω_c (see Sec. II). This would mean considerably more numerical effort, and since μ^* and T_c are virtually independent of ξ_c, we forego further improvement of this accuracy. In going from the RPA to the SRPA, the renormalization effect on the exchange interaction has to be taken into account as a further correlation contribution, and the proper quantity to be compared with is

$$\tilde{\xi}_c = \xi_c + \mathcal{X}_0^{ex}(k_F) + \Delta\mathcal{X}^{ex}(k_F) - \mathcal{X}_{00}^{ex}(k_F) , \qquad (29)$$

which is also given in Table I. $\tilde{\xi}_c$ is very close to ξ_c, so self-consistency has little influence on ξ_c in the range $0 \leq r_s \leq 5$.

We now proceed to our results for μ^* and T_c, which are listed in Table I. The calculations for μ^* were performed using a cutoff $\omega_0 = 1000$ K, which is 5–10 times the Debye temperature of the alkali metals. If a different cutoff ω_0' is to be used, μ^* has to be transformed according to

$$1/\mu^*(\omega_0') = 1/\mu^*(\omega_0) - \ln(\omega_0'/\omega_0) . \qquad (30)$$

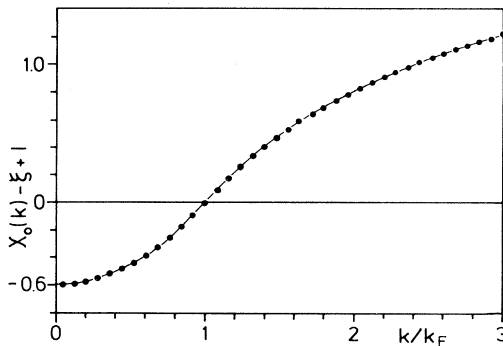Superconductivity appears whenever $\mu^* < 0$. From Eq. (24) it follows that T_c is given by

$$T_c = 1.13\omega_0 e^{1/\mu^*} \qquad (31)$$

if the electron interaction alone is responsible for superconductivity. In the SRPA, $\mu^* < 0$ for $r_s \geq 2.5$. It is instructive to consider the frequency dependence of the pseudopotential for k at the Fermi surface. In Fig. 9, the quantity

$$C_n^{k_F} \equiv -C_{n,0}^{k_F,k_F}/T$$

is plotted as a function of ω_n for $r_s = 1$ ($\mu^* > 0$) and $r_s = 4$ ($\mu^* < 0$). μ^* is related to $C_n^{k_F}$ via Eq. (25). In both cases, there is a strong reduction of $C_n^{k_F}$ from the high-frequency value to that at zero-frequency transfer, thus clearly manifesting the almost complete cancellation between static repulsion and dynamic attraction. For $r_s = 4$, exchange of virtual plasmons overcompensates repulsion and leads to superconductivity, whereas for $r_s = 1$ repulsion dominates.

Our SRPA results for μ^* are in contradiction to the experiment on the alkali metals. With the exception of Li, bandstructure effects are small in these metals, and they should be well described in terms of a free-electron gas. Since electron-phonon coupling, though weak in these metals, provides an additional pair-binding mechanism, the occurrence of a negative μ^* would result in comparatively high T_c's. For instance, for Na, $r_s \sim 4$ and in the SRPA, $\mu^* \sim -0.07$ for $r_s = 4$. Together with an electron-phonon coupling strength[22] $\lambda \sim 0.16$ and $\Theta_D \sim 160$ K, this would lead to $T_c \sim 2$ K, in striking disagreement with the
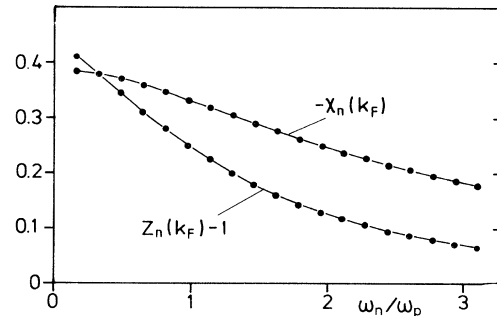

FIG. 6. Even part of the normal-state self-energy vs k for $n = 0$.

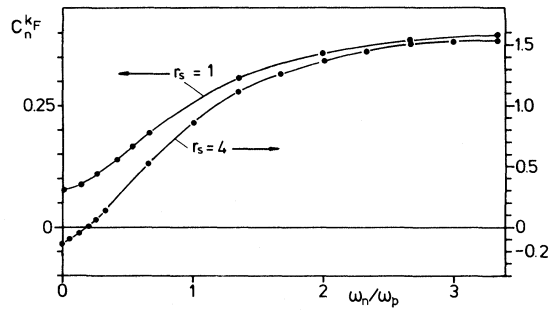FIG. 8. Even and odd parts of the normal-state self-energy vs ω_n for $k = 1.0$.

FIG. 9. Pseudopotential-$C_{n0}^{k_F k_F}/T$ vs ω_n for a cutoff $\omega_0 = 0.04 \pi \epsilon_F$.

experiment which shows no superconductivity down to the mK range. Thus, the change of sign in μ^* for $r_s > 2.5$ is clearly an indication of the inadequacy of the SRPA and proves the necessity of the inclusion of vertex corrections (spin-fluctuation-type diagrams) in the effective Cooper-pair interaction V^-. This will be left to a forthcoming paper, but we want to anticipate one major result: The consideration of vertex corrections generally leads to a flattening of V^- as a function of energy transfer [i.e., to a reduction of $\sigma(k,k')$ in Eq. (12)], and as a consequence to a μ^* which is positive over the whole range $0 \leq r_s \leq 5$.

Incidentally, we note that our numerical solution for Eq. (1a) *without* the normal-state self-energy correction yields a T_c at least an order of magnitude higher than that with the self-energy correction in the range of $r_s > 5$. This demonstrates the danger of regarding the system as weak coupling merely because $T_c \ll E_F, \omega_p$. Our T_c values for $r_s > 10$, without the self-energy correction, are 3 orders of magnitude higher than those of Takada,[12] who considered the same RPA interaction as we do but using the KMK approximation[14] to solve the Eliashberg equation (1a). Thus, the unreliability of the KMK approximation for high-frequency attractive mechanisms is demonstrated.

VI. SUMMARY AND DISCUSSIONS

For the dual purpose of studying electron-attracting mechanisms at high frequency and of investigating the contribution of the electron Coulomb interaction as embo-

died in the quantity μ^*, we adopt a well-defined model of the RPA in an electron gas. The Eliashberg equation with two variables, momentum and frequency, is solved numerically, including the self-energy correction. As a by-product, we have obtained the normal-state self-energy in the self-consistent RPA.

The T_c results show that the attraction due to plasmons within the RPA is an effective counterbalance to the low-frequency Coulomb repulsion. If we apply the electron-gas results to simple metals for $r_s < 2.5$, the net Coulomb interaction effect is to lower T_c, although the effective μ^* is lower than the common estimate for aluminium ($r_s = 2$). For lower-density metals ($r_s > 3$), the RPA predicts superconductivity due to electron Coulomb interaction alone. From these two facts we infer that the plasmon attraction is overestimated within the RPA.

The terms left out of the RPA for the Cooper-pair interaction include the vertex corrections and the crossed diagrams[5] (electron-hole ladders responsible for the spin fluctuations). We have found that static approximations[20,23,24] to these terms depress T_c and, hence, increase μ^* drastically. However, since the frequency dependence of the Cooper-pair interaction is important, these static approximations may have overestimated the effects of the corrections to the RPA. Therefore, we plan a more careful investigation of μ^* in the electron gas beyond the RPA.

The plasmon attraction is very similar in structure to the exciton mechanism.[13,15] Even though T_c is very small compared to the typical plasmon or exciton frequency, it is misleading to regard the resultant superconductivity as weak coupling, in the sense that self-energy and vertex corrections are not negligible. Our calculations show that neglecting these terms may lead to an overly optimistic estimate of the superconducting transition temperature due to the high-frequency attraction.

[1]D. Rainer, in Proceedings of the XXth International Conference on Low Temperature Physics, Los Angeles, 1981, edited by W. G. Clark [Physica <u>109 & 110B</u>, 1671 (1982)].

[2]P. B. Allen and B. Mitrović, in *Solid State Physics*, edited by H. Ehrenreich, F. Seitz, and D. Turnbull (Academic, New York, 1982), Vol. 37, p. 1.

[3]C. M. Varma, in *Superconductivity in d- and f-Band Metals 1982*, edited by W. Buckel and W. Weber (Kernforschungszentrum Karlsruhe GmbH, Karlsruhe, 1982), p. 603.

[4]D. J. Scalapino, in *Superconductivity*, edited by R. D. Parks (Dekker, New York, 1969), Vol. 1, p. 449.

[5]G. Gladstone, M. A. Jensen, and J. R. Schrieffer, in *Superconductivity*, edited by R. D. Parks (Dekker, New York, 1969), Vol. 2, p. 665.

[6]W. L. McMillan, Phys. Rev. <u>167</u>, 331 (1968).

[7]W. L. McMillan and J. M. Rowell, in *Superconductivity*, edited by R. D. Parks (Dekker, New York, 1969), Vol. 1, p. 561.

[8]F. J. Culetto and F. Pobell, Phys. Rev. Lett. <u>40</u>, 1104 (1978).

[9]D. Glötzel, D. Rainer, and H. R. Schober, Z. Phys. B <u>35</u>, 317

(1979).

[10]H. Rietschel, H. Winter, and W. Reichardt, Phys. Rev. B 22, 4284 (1980).

[11]For a recent review of acoustic plasmons, see J. Ruvalds, Adv. Phys. 30, 677 (1981).

[12]Y. Takada, J. Phys. Soc. Jpn. 45, 786 (1978).

[13]For a thorough review of the literature on this subject, see *High-Temperature Superconductivity,* edited by V. L. Ginzburg and D. A. Kirzhnits (Consultants Bureau, New York, 1982).

[14]D. A. Kirzhnits, E. G. Maksimov, and D. I. Khomskii, J. Low Temp. Phys. 10, 79 (1973).

[15]D. Davis, H. Gutfreund, and W. A. Little, Phys. Rev. B 13,

4766 (1976).

[16]B. Schuh and L. J. Sham, J. Low Temp. Phys. 50, 391 (1983).

[17]G. D. Mahan, *Many-body Physics* (Plenum, New York, 1981), p. 387.

[18]L. Hedin, Phys. Rev. 139, A796 (1965).

[19]D. F. Dubois, Ann. Phys. 7, 174 (1959).

[20]A. W. Overhauser, Phys. Rev. B 3, 1888 (1971).

[21]S. H. Vosko, L. Wilk, and M. Nusair, Can. J. Phys. 58, 1200 (1980).

[22]G. Grimvall, Phys. Scr. 14, 63 (1976).

[23]N. Iwamoto and D. Pines (private communication). We are grateful to Professor Pines for a discussion of their work.

[24]P. Vashishta and K. S. Singwi, Phys. Rev. B 36, 875 (1972).